Eurographics Workshop on 3D Object Retrieval (2008)
I. Pratikakis and T. Theoharis (Editors)

3D Object Retrieval based on Resulting Fields

A. Mademlis[1] P. Daras[2] D. Tzovaras[2] M.G. Strintzis[1]

[1] Information Processing Labaratory
Department of Electrical & Computer Engineering
Aristotle University of Thessaloniki
Thessaloniki 54006 Greece

[2] Informatics and Telematics Institute
Centre for Research and Technology Hellas
1st km Thermi Panorama Rd, PO Box 60361
57001, Greece

Abstract

3D object search and retrieval has become a very challenging research field over the last years with application in many areas like computer vision, car industry, medicine, etc. All approaches that have been proposed so far are based on the analysis of the shape of the 3D object, either concerning its surface or its volume. In this paper, a completely different approach is followed: Instead of extracting features from the 3D object, its shape's "impact" on the surrounding area is examined. This impact is expressed by considering the 3D object voxels as electric point charges and computing the resulting electrostatic field in a neighborhood around it. The proposed approach ensures robustness with respect to object's degeneracies and native invariance under rotation and translation. Experiments which were performed in a 3D object databases proved that the proposed method can be efficiently used for 3D object retrieval applications.

Categories and Subject Descriptors (according to ACM CCS): I.3.3 [Computer Graphics]: Line and Curve Generation

1. Introduction

3D object retrieval is a relatively new and challenging research field and a major effort of the research community has been devoted to the creation of accurate and efficient 3D object search and retrieval algorithms.

Generally, descriptor extraction procedures focus on the description of geometry of the 3D object for almost all approaches presented so far. The commonly utilized descriptors are global features, local features, histograms, graphs or combinations of the above [TV04, BKSS07].

Two are the main problems that pose obstacles in the efficiency of the algorithms that have been proposed so far: The object degeneracies (holes, missing polygons, etc) and the pose normalization. The first problem is usually tackled by applying a triangulation algorithm (e.g. Delaunnay) or a hole filling algorithm [WPK*04]. Concerning the second one, two widely acceptable solutions have been proposed: the description of the object in a natively rotation invariant form and the rotation normalization of the object in a preprocessing step. Both approaches present advantages and drawbacks: The rotation normalization [Vra03] ensures that very highly discriminant descriptors can be computed, however it can not guarantee that all the similar objects will be normalized in a similar manner. In contrast, the utilization of natively rotation invariant descriptors [KFR03] which avoids the rotation normalization problems, usually results in descriptors which are not very highly discriminant.

The major contribution of this paper is a new perspective in 3D object description. The descriptors of the 3D object are not derived directly from its geometry. Instead, the results of the insertion of the object in the space have been chosen to describe the 3D object. More specifically, the 3D object is treated as an electric charge or a newtonian mass positioned in the empty space. Then, the resulting field is computed and novel descriptors are extracted from it. The field is described using expansions of the traditional Newtonian and Coulomb laws. By doing so, the proposed method is robust to object's degeneracies and produces a fusion of local and global translation and rotation invariant descriptors, with high discriminant power.

The rest of the paper is organized as follows. In Section 2 the descriptor extraction process is presented. More specif-

ically, the implemented field theory is described in subsection 2.1 and the histogram computation in subsection 2.2. The matching method is described in Section 3, while the experimental results are discussed in Section 4. Finally, the conclusions are drawn in Section 5.

2. Descriptor Extraction

Let us assume that a 3D object is described as a binary volumetric function normalized with respect to scaling. If the object is described in another form (e.g. polygon mesh), a preprocessing step that transforms the object in a binary volumetric function is imposed [DZTS06].

The key idea of the proposed approach is the description of the resulting phenomena occurred by the insertion of the 3D object in the space. It is expected that similar objects will result in similar physical phenomena. Some obvious selections are the traditional electrostatic force field (following the Coulomb law) and the Newtonian force field. More sophisticated selections could involve the generalized Einstein field theory, or the Maxwell electromagnetic field theory. The present paper focuses on static fields inspired from the traditional Newton and Coulomb laws.

2.1. Field Computation

In order to compute a field, a cause for the field existence should be selected. Thus, every voxel of the 3D object is considered as point mass $m[n,m,l]=1$, (or, equivalently as a point charge $q[n,m,l]=1$). Any 3D object can be considered as a distributed mass (or a distributed charge) with a specific distribution, resulting in a static field around it. More specifically, in every point $\mathbf{x}=[x\ y\ z]^T$ of the 3D space that is not occupied by the object, the density and the potential of the field can be computed according to:

$$\mathbf{E}(\mathbf{x}) = C\sum_{i=0}^{N}\frac{1}{|\mathbf{x}-\mathbf{x}_i|^3}(\mathbf{x}-\mathbf{x}_i) \quad (1)$$

$$\phi(\mathbf{x}) = C\sum_{i=0}^{N}\frac{1}{|\mathbf{x}-\mathbf{x}_i|} \quad (2)$$

where $\mathbf{E}(\mathbf{x})$ is the density of the force field, $\phi(\mathbf{x})$ is the potential of the field, C is a constant value and $\mathbf{x}_i$ are the points of the 3D space that are occupied by the object.

The field described using (1) and (2) is the classical Newtonian (or equivalently the Coulombian) field. In order to achieve better discrimination, for the needs of the present paper, the field has been generalized as:

$$\mathbf{E}(\mathbf{x}) = \sum_{i=0}^{N}\frac{1}{|\mathbf{x}-\mathbf{x}_i|^{R+1}}(\mathbf{x}-\mathbf{x}_i) \quad (3)$$

$$\phi(\mathbf{x}) = \sum_{i=0}^{N}\frac{1}{|\mathbf{x}-\mathbf{x}_i|^{R-1}} \quad (4)$$

where $R=1,2,\ldots$ is a free parameter that defines the field's law. It is obvious that for $R=2$, the generalized field is identical to the classical Newtonian/Coulombian field. The constant parameter has been selected to be $C=1$, without any loss of generality.

The field is computed in various points in the exterior of the object. It can easily be proved that the field values of the points that are closer to the object present more differences (and thus, are more discriminative), when compared to the field values on points that are away, due to the factor $|\mathbf{x}-\mathbf{x}_i|$ in the denominator of equations (3) and (4). The field, which tends to be homogenous as the point is moved away from the object, is clearly depicted in the equipotential areas around the object (Fig 1).

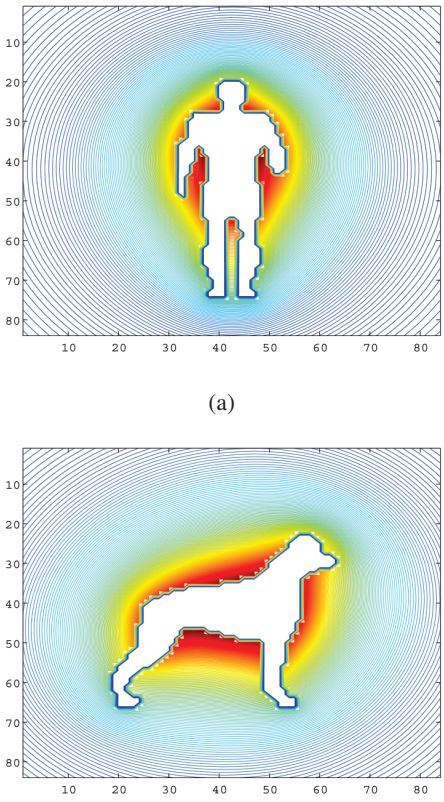

(a)

(b)

Figure 1: *The field's potential $\phi(\mathbf{x})$ produced from (a) human and (b) animal.*

2.2. Histogram Computation

The field descriptor, in the proposed approach, is composed of three major histograms created by:

- The field potential values, computed in points that are equidistant from the object surface.

$$\left\{\phi(\mathbf{x}) : \mathbf{x} \in R^3, \min_{\mathbf{x}_i}(\mathbf{x}-\mathbf{x}_i) = d\right\} \quad (5)$$

- The field density Euclidean norms, computed in points that are equidistant from the object surface.

$$\left\{|\mathbf{E}(\mathbf{x})| : \mathbf{x} \in R^3, \min_{\mathbf{x}_i}(\mathbf{x}-\mathbf{x}_i) = d\right\} \quad (6)$$

- The radial component of the field density, computed in points that are equidistant from the object surface.

$$\left\{\mathbf{E}(\mathbf{x}) \cdot \mathbf{n}_r(\mathbf{x}) : \mathbf{x} \in R^3, \min_{\mathbf{x}_i}(\mathbf{x}-\mathbf{x}_i) = d\right\} \quad (7)$$

where $\mathbf{n}_r(\mathbf{x}) = \frac{\mathbf{x}-\mathbf{x}_c}{|\mathbf{x}-\mathbf{x}_c|}$ and $\mathbf{x}_c$ is the mass center of the 3D object

The computation of the histograms involves only relative distances, thus the resulting histograms are completely invariant under rotation and translation of the 3D object. Thus, every object has to be normalized with respect to scaling which is achieved by scaling the 3D object so as its bounding sphere has a predefined radius.

3. Matching Method

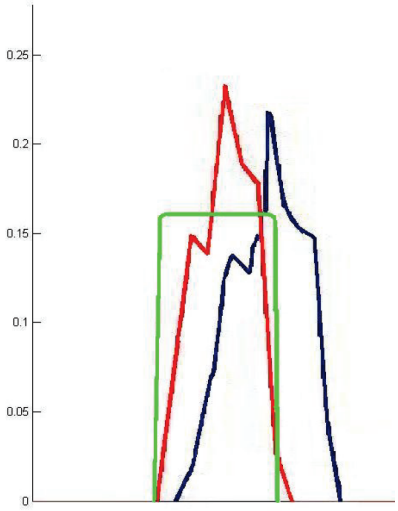

Figure 2: *Three histograms: H_1: blue, H_2: red, H_3: green*

The matching method of the presented approach is based on histogram metrics. The widely adopted L_n Minkowski distance is not a sufficient dissimilarity metric. Generally, the histograms present differences and require special metrics. The need for more sophisticated metrics can be clearly depicted in Figure 2, where two histograms of similar objects are presented along with a different histogram. Intuitively, the distance between the histograms H_1 and H_2 should be smaller than the difference between H_1 and H_3. However, the distances computed using traditional metrics (e.g. Minkowski L_1) leads to completely different results. A more comprehensive study concerning histogram comparison can be found in [LO06]. For the needs of this paper, the following metrics have been utilized:

- The normalized distance, presented in [DZTS06], which is computed as:

$$d(H_1,H_2) = \sum_{i=1}^{K} \frac{2|H_1(i)-H_2(i)|}{H_1(i)-H_2(i)} \quad (8)$$

where K is the number of histogram bins

- The diffusion distance [LO06] where the difference between two histograms H_1 and H_2 is treated as an isolated temperature field and a metric for its diffusion is computed.

For every histogram, due to their different nature, a different comparison metric has been utilized. More specifically, for the potential related histograms the normalized distance of (8) has been utilized, and the diffusion distance of [LO06], for the other two types of histograms.

4. Experimental Results

The proposed approach has been evaluated for its retrieval performance in the database presented in [DZTS06] and compared to the approaches proposed in [KFR03, Vra03, COT*03]. Every object is described as a binary volumetric function in a $N \times N \times N$ grid with $N = 64$. Each object descriptor is composed of eight histograms of potential values, eight histograms of field's density and eight histograms of field's radial component for $R = 1,2,5,6$ field's laws, examined at points that are $d = 1$ and $d = 2$ far from the object surface. Every histogram is composed by 75 bins.

The distance between the object's surface and the examined points was kept considerably small in order to capture the differences in the field values which can be examined easier for the points that are closer to the object surface. Furthermore, the values of R have been properly chosen so as both global and local features to be captured. Specifically, for $R = 1,2$, the potential and the density of the field depend on the global shape of the object, while for $R = 5,6$, the factor $|\mathbf{x}-\mathbf{x}_i|$ in the denominator of equations (3) and (4) it is ensured that the computed values mainly depend on the local objects features. Thus, in the same descriptor, a fusion of local and global features is achieved.

The object descriptors are compared in pairs. Every descriptor is divided into 24 histograms, and is compared to the appropriate histogram of the other object and "sub-dissimilarities" are computed using the dissimilarity metrics presented in Section 3. The final dissimilarity metric between two objects is the summation of the sub-dissimilarities.

The retrieval performance of the proposed approach has been evaluated using the precision-recall diagrams, where precision is the ratio of the similar retrieved objects divided to the total number of the retrieved objects, and recall is the ratio of the similar retrieved objects divided to the total number of similar objects in the database.

The mean time required for the descriptor extraction was about 30 seconds, measured in an Intel Pentium 3.2 GHz, running Windows XP.

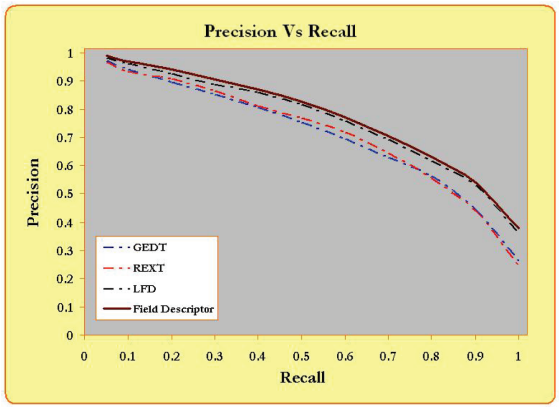

Figure 3: *Precision Recall Diagrams of the methods LFD [COT*03], REXT [Vra03], GEDT [KFR03] and the proposed approach(Field)*

The retrieval performance of the presented method has been compared to the Light Field Descriptor(LFD) [COT*03], the Radialized spherical Extent Function (REXT) [Vra03] and the Gaussian Euclidean Distance Transform (GEDT) [KFR03]. The comparative results are presented in Figure 3.

The presented results prove the highly discriminative nature of the obtained information. This can be intuitively explained by:

- *The fusion of global and local features*: The global features provide general information about the object while local features justify the result.
- *The nature of the descriptors*: The static field that has been considered around every object is unique for every object and extends it. The information of the 3D object's descriptors is captured indirectly and is natively invariant to degeneracies and common geometrical transformations (translation and rotation).

5. Conclusions

In this paper, a novel approach for 3D shape comparison was proposed. The main contribution of the proposed approach is the novel prospect in the 3D object descriptor. The extracted histogram descriptors captured the 3D geometry information indirectly, by examining the 3D objects resulting field. The traditional Newtonian / Coulombian field equations were extended in order to produce histogram descriptors capable of capturing both global and local feature information. The matching method was based on histogram dissimilarity metrics. Every 3D object's descriptors are composed of both local and global features, obtained using different parameters in the field's equations. The experimental results proved that the proposed approach outperforms other well known algorithms that have been presented in the literature.

6. Acknowledgements

This work was supported by the ***VICTORY*** (http://www.victory-eu.org) and ***CATER*** (http://www.cater-ist.org/) EC projects and by the PENED 03ED36 project co-funded 75% by EC and 25 % by the Greek General Secretariat for Research and Technology

References

[BKSS07] BUSTOS B., KEIM D., SAUPE D., SCHRECK T.: Content-based 3d object retrieval. *IEEE Computer Graphics and Applications 27*, 4 (2007), 22–27.

[COT*03] CHEN D.-Y., OUHYOUNG M., TIAN X.-P., SHEN Y.-T., , OUHYOUNG M.: On visual similarity based 3d model retrieval. In *Eurographics* (Granada, Spain, 2003), pp. 223–232.

[DZTS06] DARAS P., ZARPALAS D., TZOVARAS D., STRINTZIS M. G.: Efficient 3-d model search and retrieval using generalized 3-d radon transforms. *IEEE Transactions on Multimedia 8*, 1 (2006), 101–114.

[KFR03] KAZHDAN M., FUNKHOUSER T., RUSINKIEWICZ S.: Rotation invariant spherical harmonic representation of 3D shape descriptors. In *Symposium on Geometry Processing* (June 2003).

[LO06] LING H., OKADA K.: Diffusion distance for histogram comparison. In *CVPR '06: Proceedings of the 2006 IEEE Computer Society Conference on Computer Vision and Pattern Recognition* (Washington, DC, USA, 2006), IEEE Computer Society, pp. 246–253.

[TV04] TANGELDER J. W. H., VELTKAMP R. C.: A survey of content based 3d shape retrieval methods. In *SMI '04: Proceedings of the Shape Modeling International 2004 (SMI'04)* (Washington, DC, USA, 2004), IEEE Computer Society, pp. 145–156.

[Vra03] VRANIC D. V.: An improvement of rotation invariant 3d-shape based on functions on concentric spheres. In *ICIP (3)* (2003), pp. 757–760.

[WPK*04] WEYRICH T., PAULY M., KEISER R., HEINZLE S., SCANDELLA S., GROSS M.: Post-processing of scanned 3d surface data. In *Eurographics* (Granada, Spain, 2004)).